A Compact Multi-Probe Reverberation Chamber for Over-the-Air Testing

Wenjun Qi, Feng Fang, Wenjun Xia, Yongjiu Zhao, Lei Xing, and Qian Xu*

College of Electronic and Information Engineering
Nanjing University of Aeronautics and Astronautics, Nanjing 211106, China
qiwenjun@nuaa.edu.cn, *emxu@foxmail.com

Abstract ─ In this paper, a compact multi-probe reverberation chamber (RC) is proposed for over-the-air (OTA) testing. 16 probe antennas are used to reduce the measurement time. Typical parameters of the RC, such as field uniformity (FU), quality factor (*Q* factor), and independent samples are given. Total radiated power (TRP) and pattern correlation measurements have been performed to validate the RC system.

Index Terms ─ Compact, multi-probe RC, OTA.

I. INTRODUCTION

Reverberation chamber (RC) is an electrically large shielded cavity, which utilizes the rotation of mechanical stirrers to create a statistically uniform, isotropic, and randomly polarized fields [1-2]. Initially, an RC was widely applied to electromagnetic compatibility (EMC) testing [3-4].

With the development of the fifth-generation (5G) wireless system and various discoveries of new statistical electromagnetics in recent years, researchers have introduced RC into over-the-air (OTA) wireless device testing gradually [5]. In contrast with multi-probe anechoic chamber (MPAC) [6] and radiated two-stage (RTS) [7], RCs are more cost-effective and has larger test area in some applications. Thus, well-developed standards have been proposed in industry for OTA testing, such as IEC 61000-4-21and CTIA [8, 9]. RC has been generally used to perform total radiated power (TRP), total isotropic sensitivity (TIS), pattern correlation, diversity gain, throughput measurements of a device under test (DUT), and other fields [10-13]. Typical simulation methods of an RC are Monte-Carlo method, time domain simulation, and frequency domain simulation [14-16].

In previous work, multi-probe systems are generally used to evaluate the performance of RC or anechoic chamber (AC) [17-20]. In this paper, a compact multi-probe RC for OTA testing is designed and fabricated to meet the needs of large scale and rapid measurement of wireless devices. Compared with conventional RCs equipped with limited receiving (Rx) antennas [8], multi-probe Rx antennas can measure more samples rapidly and enhance the testing efficiency. A vertical stirrer is also used to have a hybrid stirring.

Section II presents the parameters of the proposed RC. A brief introduction of measurement setup and results are shown in Section III. Finally, Section IV concludes this article.

II. DESIGN AND ANALYSIS

The design of the proposed RC is introduced in Fig. 1, with internal dimensions of 0.6 m×0.45 m ×0.46 m. 16 probe antennas are optimized to have a good isolation and are placed on the walls of the RC. A radio frequency (RF) switch is used to switch received power from different probes. In this section, typical figures of merit: field uniformity (FU), quality factor (*Q* factor), independent sample number of the multi-probe RC are investigated to characterize its performance.

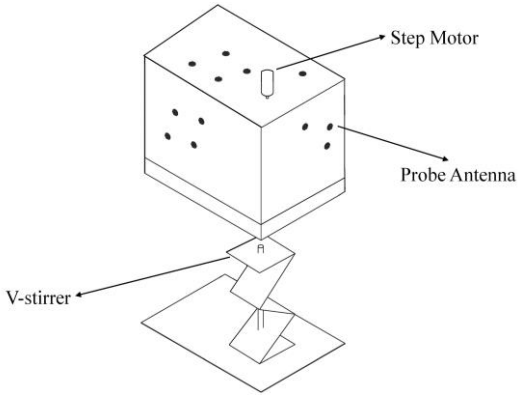

Fig. 1. The multi-probe RC, the inner dimensions are 0.6 m×0.45 m×0.46 m.

A. Field uniformity

The FU is a fundamental parameter of an RC, which characterizes the statistical uniformity of an RC. It is defined as the relative standard deviation of the maximum values obtained at the eight positions in RC [2]. When the standard deviation (dB) is lower than the field uniformity tolerance requirements given in [8], the field in RC can be regarded as statistically uniform. The

Submitted On: June 24, 2021
Accepted On: August 24, 2021
https://doi.org/10.47037/2021.ACES.J.360911

lowest usable frequency (LUF) is the lowest frequency, which occurs three to six times the first chamber resonance f_{1st}. The f_{1st} is 410MHz and the theoretical LUF is about 1.23 GHz~2.46 GHz. The possible mode is 72, which meets the requirements in the RC [8].

In this measurement, transmitting (Tx) antenna is placed at 5 different positions within the corner and the center of the working volume, as shown in Fig. 2. In Fig. 3, the FUs obtained from the mean received power (P_r) and the maximum P_r, are lower than the FU tolerance from 0.94 GHz to 14 GHz. Furthermore, the LUF is 0.94GHz, lower than the theoretical value, which means the multi-probe Rx antennas system enhances the stirring efficiency.

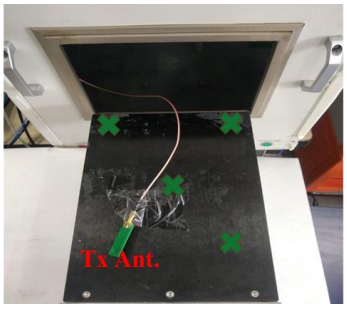

Fig. 2. FU measurement setup.

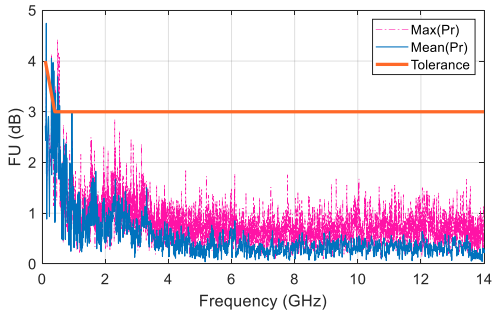

Fig. 3. The FU in the RC compared with the tolerance requirements.

B. Quality factor

Q factor represents the ability of a cavity to store energy, which is defined as the ratio of the dissipated power P_t to the stored power U:

$$Q = \frac{\omega U}{P_t}. \tag{1}$$

Here, we use the time domain (TD) method to calculate Q factor [2]. The chamber decay constant τ_{RC} is obtained from the trace of the received power in TD, thus Q factor can be calculated from:

$$Q = \omega \tau_{RC}, \tag{2}$$

where ω is the angular frequency. The coherence bandwidth Δf can be obtained as:

$$\Delta f = \frac{f}{Q}, \tag{3}$$

where f is the frequency of interest. The τ_{RC}, Q factor and Δf are demonstrated in Figs. 4 (a) and (b), which can be changed through different loading conditions. An appropriate value in RC is useful to realize a stable link for OTA testing.

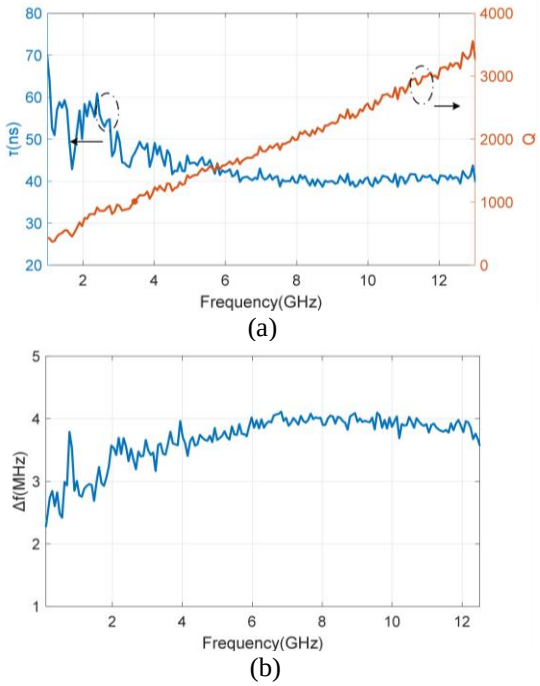

Fig. 4. Measured τ_{RC} , Q factor and Δf in the RC.

C. Correlation coefficient and independent sample number

To calculate the correlation coefficient among the probe antennas, we select two of 16 probes randomly, with a total of 120 combinations. The correlation coefficients from 1 GHz to 14 GHz are given in Fig. 5. When the frequency is larger than LUF, the R among typical groups is almost stable below 0.37, indicating that the probe antennas are mutually independent.

Then, the correlated angle and independent sample number for the V-stirrer are calculated. The correlation coefficient is to assess the performance of the stirrer, which is obtained as [8]:

$$\rho(\theta) = \frac{\frac{1}{n-1}\sum_{i}^{n}(x_i - u_x)(y_{\theta,i} - u_y)}{\sqrt{\frac{\sum_{i}^{n}(x_i - u_x)^2}{n-1}\frac{\sum_{i}^{n}(y_{\theta,i} - u_y)^2}{n-1}}}, \tag{4}$$

where n is the sample number over one rotation period, x_i is the received power at each stirrer position, $y_{\theta,i}$ is a shifted version of x_i by angle θ, u_x and u_y are averaged

received powers. The correlated angle $\Delta\theta$ is decided by a threshold $e^{-1} \approx 0.37$. The independent sample number N_{Ind} is $360/\Delta\theta$. The results are shown in Fig. 6.

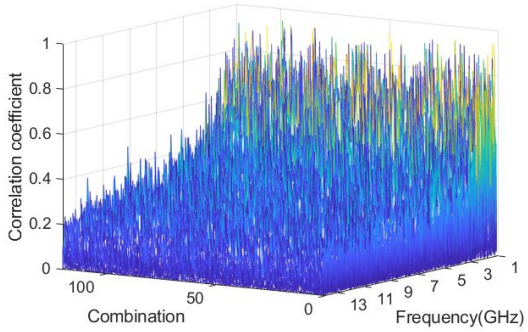

(a)

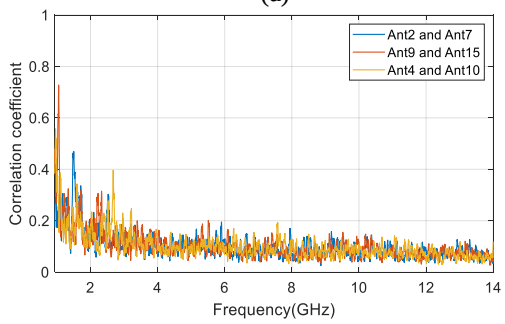

(b)

Fig. 5. The correlation coefficient between different probe antennas from 1 GHz to 14 GHz.

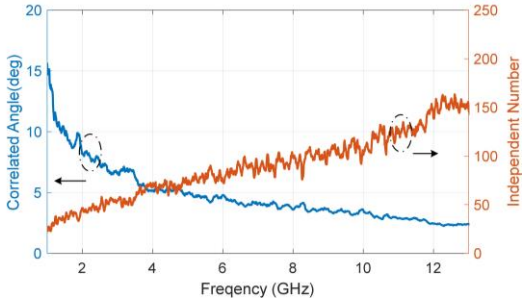

Fig. 6. Correlated angle and independent sample number.

D. *K*-Factor

The *K*-factor is the ratio between the direct power and the stirred power in RC [21]. When *K*=0, the channel is an ideal Rayleigh channel. To improve the accuracy of measurement, it is optimal to decrease the contribution of direct power. In this measurement, the *K*-factor is obtained from (5),

$$K = \frac{\left|\langle S_{21}\rangle\right|^2}{\left\langle\left|S_{21} - \langle S_{21}\rangle\right|^2\right\rangle}. \tag{5}$$

S parameters (16 × 180=2880) for different frequencies are measured between the Tx antenna and the Rx antenna. The measured *K*-factor is illustrated in Fig. 7, *K*-factors with typical probe 1, 7 and 9 are given, *K*-factor with hybrid stirring is also presented. Note that the mean value of the *K*-factor is lower than -20 dB using a hybrid stirring in the frequency range of (1 GHz -13 GHz), which means an equivalent high total scattering cross section is achieved (i.e., high stirring efficiency).

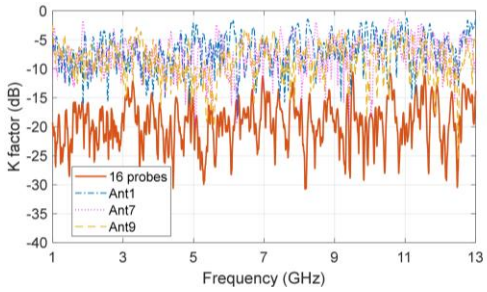

Fig. 7. Measured *K*-factors in the RC.

III. MEASUREMENTS AND RESULTS

A. Total radiated power

TRP is one of the performance indicators in OTA testing, which usually reflects the transmitted power of wireless devices. Here, we utilize multi-probe RC to realize fast and accurate measurements in 5G FR1 band.

As shown in Fig. 8, the test procedure of TRP is as follows:

1. Conduct the transfer function characterization procedure with the reference power [8].

2. Put the DUT (a WIFI device) into the RC. With the power meter and RF switch, measure and record 16 powers received by different probe antennas in each stirring sample.

3. TRP can be calculated from (6):

$$P_{\mathrm{TRP}} = \frac{1}{N}\frac{\sum_{n=1}^{N} P_n}{G_{\mathrm{ref}} e_{\mathrm{mismatch,meas}} \eta_{\mathrm{meas}} G_{\mathrm{cable}}}, \tag{6}$$

where N is the total sample number, P_n is the nth measured power, G_{ref} is the power transfer function, G_{cable} is the loss of the cable and $e_{\mathrm{mismatch,meas}}$ is the antenna mismatch factor.

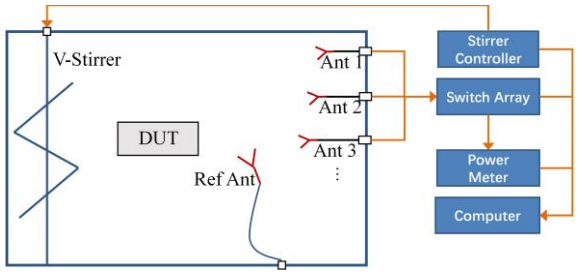

Fig. 8. Configuration of the multi-probe RC for TRP measurement.

We recorded 720 power values (8° one step and 45 stirrer positions) at 2.4 GHz and 5.18 GHz. When the V-stirrer rotates once, the RF switch turns to 16 probe antennas in sequence, therefore, 16 samples can be measured in one step. Multi-Probe could obtain 16 samples within 2.1 seconds, while conventional probe in RC needs 128 seconds. It only takes 5 minutes to get 720 samples. Thus, the method can effectively decrease the testing time and obtain much more samples rapidly and accurately in the same period.

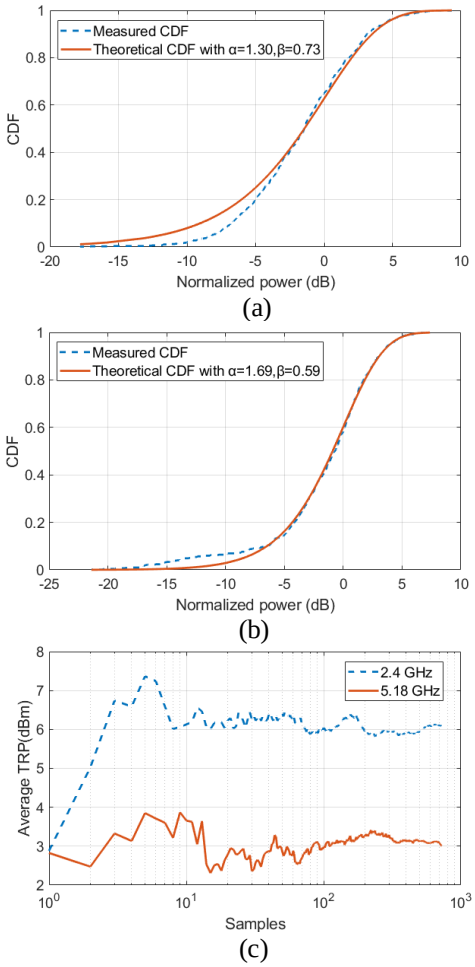

Fig. 9. (a) CDFs of the measured and theoretical normalized power samples at 2.4 GHz; (b) 5.18 GHz; (c) average TRP at 2.4 GHz, 6.03 dBm and 5.18 GHz, 3.00 dBm.

The bandwidth of signal transmitted from DUT is not much larger compared with the coherence bandwidth of the proposed RC shown in Fig. 4 (b) [22]. So that, the cumulative distribution function (CDF) of the measured normalized power *p(x)* is gamma distribution in (7):

$$p(x) = \frac{(1/\beta)^{\alpha}}{\Gamma(\alpha)} x^{\alpha-1} e^{-x/\beta}, \tag{7}$$

where $\alpha \approx \mathrm{BW}/\Delta f$, BW is the bandwidth of the signal, β is the mean value of measured power samples.

As shown in Figs. 9 (a)-(c), the measurement results agree well with the theoretical CDF at 2.4 GHz and 5.18 GHz. We also calculate average TRP of DUT in the above frequency. The theoretical lower limit of σ_{rTRP} is 4.21% at 2.4 GHz, 4.17% at 5.18 GHz.

B. Pattern correlation

The pattern correlation can be used to check the antenna status for a DUT with multiple antennas. Suppose we have a reference device (which we know the performance is good), by comparing the pattern correlations between the DUT antenna and the reference device (with the same port), we can identify the similarity between the radiation pattern of the DUT and the reference. If the pattern correlations deviate from reference values significantly, there should be something wrong for the antenna performance.

According to the conclusions given in [11], the angular correlation can be defined over the measured received power. Therefore, we can calculate the pattern correlation by the received powers of the multi-probe antennas. The testing setup of pattern correlation is similar to the measurement of TRP. The only distinction is that the pattern correlation measurement does not need a reference antenna. The procedure is executed using the following steps:

1. Place the reference device into the valid test volume of the chamber. Turn on the power meter, the measured radiated powers for all probe antennas and each mode-turn sample can be obtained, which is $P_{11}, P_{12}, \ldots P_{1n}$ (n represents mode-stirring numbers).

2. Replace the reference device with the DUT in the same position. Rotate the mode-stirring paddle as the same sequence determined by the standard-part procedure. The measured radiated powers $P_{21}, P_{22}, \ldots P_{2n}$ can be received.

3. Calculate the value of radiated pattern correlation R by taking an average of all power samples and formula (8):

$$R = \frac{\frac{1}{n-1}\sum_{i}^{n}(P_{1i} - \langle P_1 \rangle)(P_{2i} - \langle P_2 \rangle)}{\sqrt{\frac{\sum_{i}^{n}(P_{1i} - \langle P_1 \rangle)^2}{n-1}\frac{\sum_{i}^{n}(P_{2i} - \langle P_2 \rangle)^2}{n-1}}}, \tag{8}$$

where P_n is the measured power for the n_{th} sample and N is the total number of mode-stirring samples, $\langle P_1 \rangle$ and $\langle P_2 \rangle$ are the average of the standard part and DUT total mode-stirring samples respectively. As shown in Fig. 10 (a), the pattern correlation coefficient R is close to 1, therefore DUT1 works well as expected. In (b), there should be something wrong of antenna 1 in DUT2.

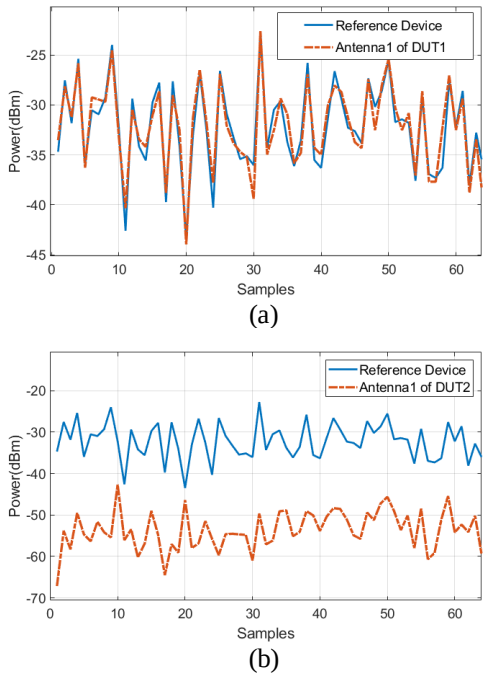

Fig. 10. Pattern correlation between different antennas: (a) R=0.9520; (b) R=0.1552.

IV. CONCLUSION

A compact multi-probe RC is manufactured in this paper. Typical figures of merit in the compact multi-probe RC are presented to assess the performance of RC. The FU satisfies the FU tolerance in [8] and the LUF is about 0.94 GHz. The correlation coefficient shows that 16 probe antennas are independent of each other.

We have shown that when the radiated spectrum is wider than the coherence bandwidth, the measured TRP has a Gamma distribution in the frequency band of 2.4 GHz and 5.18 GHz. The average TRP and σ_{rTRP} have been measured. The proposed system is very efficiency, in the TRP measurement, the measurement duration of 16 samples is about 2.1 seconds (with 0.13 s/sample). The pattern correlations between different antennas of the DUTs have also been measured.

ACKNOWLEDGMENT

This work was supported in part by the Fundamental Research Funds for the Central Universities (No. NS2021029), and in part by the National Natural Science Foundation of China under Grants 61701224 and 61601219.

REFERENCES

[1] D. A. Hill, *Electromagnetic Fields in Cavities: Deterministic and Statistical Theories*. Hoboken, NJ, USA, 2009.

[2] Q. Xu and Y. Huang, *Anechoic and Reverberation Chambers: Theory, Design and Measurements*. Wiley-IEEE, UK, 2019.

[3] P. Corona, G. Latmiral, E. Paolini, and L. Piccioli, "Use of a reverberating enclosure for measurements of radiated power in the microwave range," *IEEE Trans. Electromagn. Compat.*, vol. EMC-18, no. 2, pp. 54-59, May 1976.

[4] W. Li, C. Yue, and W. Yu, "Study on array source stirring reverberation chamber," *Applied Computational Electromagnetics Society Journal*, vol. 29, no. 12, pp. 1067-1076, Dec. 2014.

[5] X. Chen, J. Tang, T. Li, S. Zhu, Y. Ren, Z. Zhang, and A. Zhang, "Reverberation chambers for over-the-air tests: An overview of two decades of research," *IEEE Access*, vol. 6, pp. 49129-49143, Aug. 2018.

[6] W. Fan, X. C. B. de Lisbona, F. Sun, J. O. Nielsen, M. B. Knudsen, and G. F. Pedersen, "Emulating spatial characteristics of MIMO channels for OTA testing," *IEEE Trans. Antennas Propag.*, vol. 61, no. 8, pp. 4306-4314, Aug. 2013.

[7] W. Yu, Y. Qi, K. Liu, Y. Xu, and J. Fan, "Radiated two-stage method for LTE MIMO user equipment performance evaluation," *IEEE Trans. Electromagn. Compat.*, vol. 56, no. 6, pp. 1691-1696, Dec. 2014.

[8] IEC 61000-4-21, *Electromagnetic compatibility (EMC) – Part 4-21: Testing and measurement techniques – Reverberation chamber test methods*, IEC Standard, Ed 2.0, 2011-01.

[9] CTIA, *Test Plan for Wireless Large-Form-Factor Device Over-the-Air Performance*, ver. 1.2.1, Feb. 2019.

[10] H. G. Krauthauser, "On the measurement of total radiated power in uncalibrated reverberation chambers," *IEEE Trans. Electromagn. Compat.*, vol. 49, no. 2, pp. 270-279, June 2007.

[11] Q. Xu, L. Xing, D. Yan, Y. Zhao, and Y. Huang, "Experimental verification of stirrer angular correlation with different definitions in a reverberation chamber," *the 12th International Symposium on Antennas, Propag. and EM Theory (ISAPE 2018)*, Hangzhou, China, pp. 1-5, Feb. 2018.

[12] K. Karlsson, X. Chen, J. Carlsson, and A. Skarbratt, "On OTA test in the presence of doppler spreads in a reverberation chamber," *IEEE Antennas Wireless Propag. Lett.*, vol. 12, pp. 886-889, July 2013.

[13] A. Sorrentino, G. Ferrara, and M. Migliaccio, "The reverberating chamber as a line-of-sight wireless channel emulator," *IEEE Trans. Antennas Propag.*, vol. 56, pp. 1825-1830, June 2008.

[14] Y. Cui, H. G. Wei, S. Wang, and L. Fan, "Efficient method of optimizing reverberation chamber using FDTD and genetic algorithm method," *Applied Computational Electromagnetics Society Journal*, vol. 28, no. 4, pp. 293-299, Apr. 2013.

[15] J. M. Ladbury, "Monte Carlo simulation of

reverberation chambers," *Gateway to the New Millennium. 18th Digital Avionics Systems Conference. Proceedings (Cat. No.99CH37033)*, pp. 10.C.1-10. C.1, Oct. 1999.

[16] S. Wang, Z. Wu, L. Du, G. Wei, and Y. Cui, "Study on the matrix pencil method with application to predict time-domain response of a reverberation chamber," *Applied Computational Electromagnetics Society Journal*, vol. 28, no. 9, pp. 763-771, Sep. 2013.

[17] D. Mandaris, R. Vogt-Ardatjew, E. Suthau, and F. Leferink, "Simultaneous multi-probe measurements for rapid evaluation of reverberation chambers," *2018 IEEE Intern. Symposium on Electromagn. Compat. and 2018 IEEE Asia-Pacific Symposium on Electromagn. Compat (EMC/APEMC)*, pp. 590-594, May 2018.

[18] D. Mandaris, R. Vogt-Ardatjew, M. Zaher Mahfouz, E. Suthau, and F. Leferink, "Time efficient reverberation chamber performance analysis using simultaneous multiprobe measurement technique," *Intern. Symposium on Electromagn. Compat. (EMC EUROPE)*, pp. 1-5, Aug. 2018.

[19] L. Anchidin, F. Bari, R. D. Tamas, L. Pometcu, and A. Sharaiha, "Near-field gain measurements: Single-probe distance averaging in a multipath site versus multi-probe field scanning inside an anechoic chamber," *2017 General Assembly and Scientific Symposium of the International Union of Radio Science (URSI GASS)*, pp. 1-3, Aug. 2017.

[20] J. Andersson and Z. Ying, "Analysis of different sampling methods in a reverberation chamber," *2006 First Eur. Conf. Antennas Propag. (EUCAP)*, pp. 1-5, Nov. 2006.

[21] C. L. Holloway, D. A. Hill, J. M. Ladbury, P. F. Wilson, G. Koepke, and J. Coder, "On the use of reverberation chambers to simulate a rician radio environment for the testing of wireless devices," *IEEE Trans. Antennas Propag.*, vol. 228, pp. 3167-3177, Nov. 2006.

[22] Q. Xu, W. Qi, C. Liu, L. Xing, D. Yan, Y. Zhao, T. Jia and Y. Huang, "Measuring the total radiated power of wideband signals in a reverberation chamber," *IEEE Antennas Wireless Propag. Lett.*, vol. 19, pp. 2260-2264, Oct. 2020.